Protoplasma (2013) 250:1327–1338
DOI 10.1007/s00709-013-0516-9

ORIGINAL ARTICLE

A comparative study of PNIPAM nanoparticles of curcumin, demethoxycurcumin, and bisdemethoxycurcumin and their effects on oxidative stress markers in experimental stroke

Niyaz Ahmad · Sadiq Umar · Mohammad Ashafaq · Mohd Akhtar · Zeenat Iqbal · Mohd Samim · Farhan Jalees Ahmad

Received: 21 March 2013 / Accepted: 23 May 2013 / Published online: 20 June 2013

Abstract Oxidative stress and inflammatory damage play an important role in cerebral ischemic pathogenesis and may represent a target for treatment. The development of new strategies for enhancing drug delivery to the brain is of great importance in diagnostics and therapeutics of central nervous diseases. The present study examined the hypothesis that intranasal delivery of nanoformulation of curcuminoids would reduce oxidative stress-associated brain injury after middle cerebral artery occlusion (MCAO). The rats were subjected to 2 h of MCAO followed by 22 h reperfusion, after which the grip strength, locomotor activity was performed. The effects of treatment in the rats were assessed by grip strength, locomotor activity and biochemical studies (glutathione peroxidase, glutathione reductase, lipid peroxidation, superoxide dismutase, and catalase) in the brain. Pretreatment with polymeric *N*-isopropyl acryl amide (PNIPAM) nanoparticles formulation of all three curcuminoids (curcumin (Cur), demethoxycurcumin (DMC), and bisdemethoxycurcumin (BDMC)) at doses (100 μg/kg body weight) given intranasally was effective in bringing significant changes on all the parameters. While nanoformulation of curcumin at a dose of 100 μg/kg body weight was most active in the treatment of cerebral ischemia as compared to others nanoformulation of curcuminoids. The potency of antioxidant activity significantly decreased in the order of PNIPAM nanoformulation of Cur > DMC >> BDMC, thus suggesting the critical role of methoxy groups on the phenyl ring.

Keywords Curcumin · Demethoxycurcumin · Bisdemethoxycurcumin · MCA occlusion · Oxidative stress · PNIPAM nanoparticles

Handling Editor: Damjana Drobne

N. Ahmad · Z. Iqbal · F. J. Ahmad (✉)
Nanomedicine lab, Department of Pharmaceutics,
Faculty of Pharmacy, Hamdard University,
New Delhi 110062, India
e-mail: farhanja2000@gmail.com

N. Ahmad
e-mail: niyazpharma@gmail.com

S. Umar · M. Ashafaq
Department of Medical Elemental and Toxicology,
Faculty of Science, Hamdard University,
New Delhi 110062, India

M. Akhtar
Department of Pharmacology, Faculty of Pharmacy,
Hamdard University, New Delhi 110062, India

M. Samim
Department of Chemistry, Faculty of Science,
Hamdard University, New Delhi 110062, India

Introduction

Stroke is a global public health concern and one of the leading cause of mortality and morbidity, with astronomical financial repercussions on health systems worldwide (Allen and Bayraktutan 2009; Ashafaq et al. 2012). Cerebral ischemic insult usually causes irreversible deterioration of the central nervous system (CNS) (Kim et al. 2007). After the onset of cerebral ischemia, inflammatory process triggers the acceleration of the early onset and functions as a determinant factor in severity of cerebral damage, morbidity, and mortality (Berner et al. 2005). Oxidative stress has always been implicated in the machinery of ischemia–reperfusion

injury consequently producing surplus amounts of reactive oxygen species (ROS) (Raza et al. 2011). ROS plays a role in normal physiology and is also caught up in a number of disease processes in pathological condition. A substantial body of evidence has been produced that links the production of ROS and subsequent oxidative damage to the pathogenesis of ischemia–reperfusion (Sun et al. 2009). Brain tissues are particularly susceptible to oxidative damage; therefore, it is believed that pharmacologic modification of oxidative damage is one of the most promising avenues for stroke therapy.

A number of antioxidants drugs (thioperamide, ropinirole, thymoquinone) are reported to reduce ROS-mediated reactions and rescue the neurons from reperfusion-induced neuronal loss in animal models of cerebral ischemia (Akhtar et al. 2008; Badary and Taha 2003; Iida et al. 1999). Recent in vitro and in vivo studies confirm the use of curcumin in cerebral ischemia which is chiefly found in *Curcuma longa* (Jayaprakasha et al. 2006; Thiyagarajan et al. 2004; Thiyagarajan and Sharma 2004). Curcumin (Cur), demethoxycurcumin (DMC), and bisdemethoxycurcumin (BDMC) are also reported having a potential role in the antioxidant activity (Sandur et al. 2007; Somparn et al. 2007). Curcumin exhibits low serum and tissue levels due to its poor solubility, absorption, extensive metabolism, and rapid elimination (Anand et al. 2010; Yang et al. 2007). Therefore, the therapeutic efficacy of curcumin is restricted to its short systemic retention in circulation and in tissues. To enhance the bioavailability of curcuminoids, various strategies have been applied in terms of formulations and route of administration. Blood–brain barrier (BBB) can be bypass to preferentially target the brain and to treat neurological disorders by intranasal administration of drugs (Mistry et al. 2009). Intranasal administration of curcuminoids can be effective in this regard through which blood–brain barrier can be bypassed and much higher degree of drug concentration can be achieved in the cortex, caudate-putamen, and hippocampus than intravenous administration (Hanson and Frey 2008). Therefore, we investigated formulated polymeric *N*-isopropyl acryl amide (PNIPAM) nanoparticles loaded with Cur, DMC, and BDMC through intranasal administration in middle cerebral artery occlusion-induced focal cerebral ischemia in Wistar rats.

The structure of Cur, DMC, and BDMC are shown below.

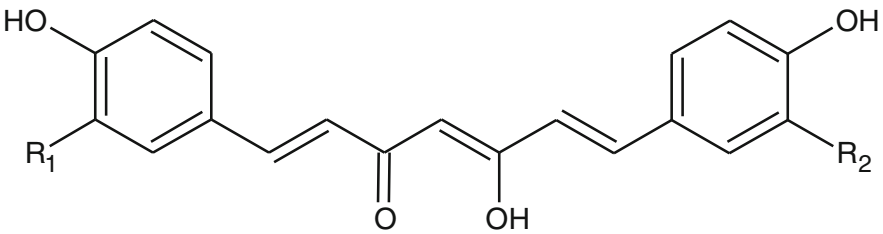

Curcuminoids (curcumin (R_1, R_2 = OCH_3), demethoxycurcumin (R_1 = H, R_2 = OCH_3), and bisdemethoxycurcumin (R_1, R_2 = H))

Materials and methods

Chemicals Cur, DMC, and BDMC (assigned purity >96 %; molecular weight 368.38, 338.36, and 308.33; melting point 183,168, and 224 °C, respectively) were purchased from LGC Promo Chem India Pvt. Ltd. Bangalore, India. A copolymer of *N*-isopropyl acrylamide (NIPAM), acrylic acid (AA), and vinylpyrrolidone (VP) was synthesized through a free radical polymerization mechanism. NIPAM was purchased from ACROS chemicals, NJ, USA; VP and AA were purchased from Sigma-Aldrich Chemicals, USA. 2,3,5-Triphenyltetrazolium chloride (TTC) and EDTA were purchased from Sigma-Aldrich Chemicals Pvt. Ltd., India.

Preparation of polymeric NIPAM NPs

Recrystallization of NIPAM was done by using hexane at room temperature. VP was freshly distilled before use and vacuum-distilled AA was used. NIPAM (85 mg), VP (10 μL), and AA (5 μL) were dissolved in water (10 mL) and polymerization was triggered by adding 20 μL of ferrous ammonium sulfate and 30 μL of ammonium persulfate solution. Twenty microliters of *N*,*N*′-methylene-bis-acrylamide (MBA) (20 mg/mL) was added for cross-linking during the polymerization reaction. The reaction was carried out at 32 °C in a N_2 atmosphere, for 28 h. After the polymerization, aqueous dispersion was dialyzed for 24 h using a spectropore

membrane dialysis bag (12 kDa cutoff; Sigma-Aldrich) and lyophilized to obtain a dry powder. Curcuminoids (Cur, DMC, and BDMC) were physically entrapped into the hydrophobic core of PNIPAM micelles by vortexing and sonication. Briefly, 10 mg PNIPAM lyophilized powder was dispersed in 2 mL of double distilled water and measured volume of ethanolic solution (1 mg/mL) of Cur, DMC, and BDMC solution was separately and gradually added. The mixture was stirred vigorously with mild sonication to give a clear aqueous solution. The different drug-loaded polymeric nanoparticles (named CUR-PNIPAM, DMC-PNIPAM, and BDMC-PNIPAM) were lyophilized to obtain a dried nanoparticle powder for therapeutic use.

Physiochemical characterization of polymeric NIPAM NPs

To determine the morphology of the prepared nanoparticles (NPs), transmission electron microscopy (TEM) was performed in which aliquots of the nanoparticle suspensions were placed on carbon-coated copper grid (Polysciences, Warrington, PA), 2 % uranyl acetate was added, and allowed to dry. TEM images were obtained by using digital imaging software—AMT Image Capture Engine (version 5.42.391). Surface morphology of the prepared NPs was studied using scanning electron microscopy (SEM) (SEM, Zeiss EVO40; Carl Zeiss, Cambridge, UK) in which the lyophilized samples were first placed in gold coating vacuum chamber and gold coating was done at 2.5 kV, 25–30 mA. Particles were observed at 25.0 kV, nominal magnification of 13,000–40,000 with scan speed = 8. The particle size, polydispersity index, and zeta potential were determined by Zetasizer Nano ZS, (Malvern Instruments Ltd, Worcestershire, UK). The lyophilized powder was dispersed in aqueous solution. Measurements were performed using standard laser 4 mW He–Ne, 633 nm, at 25 °C with a fixed angle of 90°.

Determination of loading capacity, encapsulation efficiency, and process yield of NPs

In order to quantify entrapment efficiency (EE) and loading capacity (LC) of PNIPAM NPs, the lyophilized particles were redispersed in water and were separated from unentrapped free drug using a Millipore UFP2THK24 (100 kDa cutoff) membrane filter and the amount of free drug in the filtrate was measured on a UVIKON 930 Kontron spectrophotometer (Kontron Instruments, Munich, Germany) at 450 nm. The difference between the amount of drug initially used for loading and the drug content in the filtrate was taken as an indication of the amount of drug entrapment. The entrapment efficiency and loading capacity were calculated by the following formula:

$$\textbf{Encapsulation efficiency}(\%) = (\textbf{Total drug}–\textbf{Free drug})/\textbf{Total drug} \times \mathbf{100}$$

$$\textbf{Loading capacity}(\%) = (\textbf{Total drug}–\textbf{Free drug})/\textbf{Weight of nanoparticles} \times \mathbf{100}$$

The process yield was calculated from the weight of dried NPs recovered (W1) and the sum of the initial dry weight of starting materials (W2) using the following formula:

$$\textbf{Process Yield}(\%) = \mathbf{W1}/\mathbf{W2} \times \mathbf{100}$$

Experimental animal

For neurobehavioral activity, histopathological, and biochemical estimations studies, proper approval (protocol approval no. 847) was taken from Animal Ethical Committee, Jamia Hamdard (New Delhi, India), conforming to National Guidelines on the care and use of Laboratory Animals. Wistar rats (300–400 g, 16 weeks approx. old) were kept in an environmentally controlled room (temperature 25±2 °C, humidity 45–55 %, 12 h dark–light cycle) for at least 1 week before the experiments. Animals were fed on a standard pelleted diet and water (ad libitum). The food was withdrawn 12 h before the surgical procedure. Experiments were conducted in accordance with the Animal Ethics Committee (proposal no. 847) of the Hamdard University, approved by the Government of India, New Delhi, India.

Drugs and experimental design

PNIPAM nanoparticles of Cur, DMC, and BDMC were purchased from LGC Promo Chem India Pvt. Ltd. Bangalore, India. These were dissolved in double distilled water at a dose of 100 μg/kg body wt for intranasal dosing. The dose of Cur, DMC, and BDMC were administered once 1 h before the MCAO. Rats were divided into nine groups consisting of six rats in each group. Sham operated (control), Sham + PNIPAM placebo operated (substantial control), MCAO, i.e., ischemia was induced for 2 h followed by reperfusion for 22 h, MCAO + Cur API solution, MCAO + NN_{Cur} 100 μg/kg body wt., MCAO + DMC API solution, MCAO + NN_{DMC} 100 μg/kg body wt., MCAO + BDMC API solution, and MCAO + NN_{BDMC} 100 μg/kg body wt. intranasal. After the completion of the reperfusion period, the animals were assessed for

neurobehavioral activity (locomotor and grip strength) and then sacrificed to remove brains for histopathological and biochemical estimations.

Middle cerebral artery occlusion to induce focal cerebral ischemia

The right MCAO was performed using an intraluminal filament model (Longa et al. 1989) as described by Khan et al. (2009). In brief, the rats were anesthetized with chloral hydrate (400 mg/kg, i.p.) and a silicone rubber (4 0-3033REPK10, DOCCOL, USA) coated monofilament was introduced into the external carotid artery and advanced into the middle cerebral artery (MCA) via the internal carotid artery (17–20 mm) until a slight resistance was felt. Such resistance indicated that the filament had passed beyond the proximal segment of the anterior cerebral artery. At this point, the intraluminal suture blocks the origin of MCA and occludes all sources of blood flow from the internal carotid artery, anterior cerebral artery, and the posterior cerebral artery. Two hours after the induction of ischemia, the filament was slowly withdrawn and the animals were returned to their cages. Sham group rats underwent to all surgical procedures except the MCAO. Thereafter, the animals were returned to their cages and given free access to food and water.

Postoperative care

Recovery of anesthesia took approximately 4–5 h after surgery. The rats were kept in a well-ventilated room at 25±3 °C in individual cages till they gained full consciousness and then housed one animal per cage. Food and water were kept inside the cages for the rest of 22 h so that animals could easily access it without any physical trauma due to overhead surgery.

Locomotor activity (closed field activity monitoring)

Spontaneous locomotor activity as described by Lannert and Hoyer (1998) was assessed using a digital photoactometer. Each animal was observed for a period of 10 min in a square closed arena equipped with infrared light-sensitive photocells. The apparatus was housed in a darkened, light- and sound-attenuated ventilated testing room. During activity testing, only one animal was tested at a time.

Grip strength

Grip strength meter was used as described by Ali et al. (2004) for recording the grip strength of the animal. The animal's front paws were placed on the grid of grip strength meter and were moved down until its front paws grasping the grid were released. The force achieved by the animal was then displayed on the screen and was recorded as kilogram unit.

Biochemical studies

Tissue preparation for antioxidant enzymes and glutathione assays

After behavioral study, the animals were sacrificed and their brains were taken out to give 5 % (*w*/*v*) homogenate (10 mM phosphate buffer (PB), pH 7.0 having 10 μL/mL protease inhibitors, 5 mM leupeptin, 1.5 mM aprotinin, 2 mM phenylethylsulfonyl fluoride, 3 mM peptastatin A, 0.1 mM EGTA, 1 mM benzamidine, and 0.04 % butylated hydroxytoluene) and centrifuged at 800×*g* for 5 min at 4 °C. This supernatant (S1) was used for the assay of thiobarbituric acid reactive substance (TBARS) and remaining S1 was recentrifuged at 10,500×*g* for 15 min at 4 °C (S2) to separate post-mitochondrial supernatant (PMS) which was used for the estimation of antioxidant enzymes.

Thiobarbituric acid reactive substances

TBARS, a parameter of lipid peroxidation, was measured as described by Ohkawa et al. (1979). Briefly, 0.1 mL of homogenate, 1 mL of trichloroacetic acid (10 %), and 1 mL of thiobarbituric acid (0.67 %) were added to all test tubes, covered with aluminum foil, and placed in boiling water bath for 20 min. Then, test tubes were shifted to crushed ice bath and then centrifuged at 6,000 rpm for 10 min. The absorbance of the supernatant was measured at 540 nm.

Determination of GR activity

Glutathione reductase (GR) activity was assayed by the method of Ashafaq et al. (2012) as describe by Mohandas et al. (1984). The assay system consisted of 0.1 M PB pH 7.6, 0.1 mM NADPH, 0.5 mM EDTA, 1.0 mM GSSG, and 0.1 ml PMS in a total volume of 2.0 mL. The enzyme activity was quantitated at room temperature by measuring the disappearance of NADPH at 340 nm.

Determination of glutathione peroxidase activity

Glutathione peroxidase (GPx) activity was measured according to the procedure of Mohandas et al. (1984). The reaction mixture consisted of 0.05 M PB pH 7.0, 1.0 mM EDTA, and 1.0 mM sodium azide, 1.4 U of 0.1 mL GR, 1.0 mM glutathione, 0.2 mM NADPH, 0.25 mM hydrogen peroxide, and 0.1 mL of PMS in a final volume of 2.0 mL. The disappearance of NADPH at 340 nm was recorded at room temperature. The enzyme activity was calculated as nanomole NADPH oxidized per minute per milligram protein using molar extinction coefficient of $6.22\times10^{3}\ M^{-1}\ cm^{-1}$.

Determination of catalase activity

Catalase activity was assayed by the method of Ashafaq et al. (2012). Briefly, the assay mixture consisted of 0.05 M PB pH 7.0, 0.019 M hydrogen peroxide, and 0.05 mL PMS in a total volume of 3.0 mL. Changes in absorbance were recorded at 240 nm.

Super oxide dismutase

Superoxide dismutase activity was measured by the method of Umar et al. (2012). The reaction mixture of total 1 mL consisted of 0.6 mL of phosphate buffer (0.5 M, pH 7.4), 0.1 mL PMS (10 % *w/v*), 0.1 mL xanthine (1 mM), and 0.1 mL NBT (57 mM) was incubated for 15 min at room temperature and reaction was initiated by the addition of xanthine oxidase (50 mU). The rate of reaction was measured by recording change in the absorbance at 550 nm.

Determination of protein

Protein was determined by Bradford method (Bradford 1976) using bovine serum albumin as standard.

Histopathological studies

The brains of each group of animals were perfused as described by Ashafaq et al. (2012). The brains were removed quickly and kept in the same fresh buffer containing 30 % sucrose. The brains were cut into 12-μm-thick coronal sections on a cryostat (Leica, Nußloch, Heidelberg, Germany). Every ten sections of the cortex region was mounted on glass slides and processed for hematoxylin and eosin staining.

Statistical analysis

The results of all the experiments were calculated as mean± standard error of mean (SEM). Statistical difference between the two mean values were determined by Student's *t* test for unpaired observations and analyzed by ANOVA. p values <0.05 were measured statistically significant.

Results

Preparation and characterization of PNIPAM NPs

Addition of the initiator lead to the start of the polymerization of NIPAM monomer until it reaches a certain critical length and finally it collapses giving rise to precursor particles at the temperature higher than lower critical solution temperature (LCST). The precursor particles then grow by either aggregation with the other precursor particles or are trapped by existing colloid stable particles. Moreover, the average particle sizes of PNIPAM nanoparticles are measured as a function of increasing temperature, i.e., when the temperature is raised above the LCST, the polymer undergoes a phase transition and hydrophilic random coil state collapses to form a globular hydrophobic state (Naha et al. 2009; Xu et al. 2006). We have prepared 45 placebo formulations in combination of different ratios of NIPAM, VP, AA, and MBA. We selected only four formulations in which we studied particle size, polydispersity index (PDI), zeta potential, entrapment efficiency, loading capacity, and process yield of different three curcuminoids separately. After that, we selected finally one placebo formulation for therapeutic study (formulation code D_3) (Table 1).

Table 1 Optimization of placebo nanoparticles (PNIPAM NPs) on the basis of NIPAM, VP, AA, and MBA ratio

Formulation code	% of NIPAM	% of VP	% of AA	Concentration of MBA (mg/mL)	Volume of MBA (μL)	Mean particle size (nm)±SD	Mean PDI±SD	Process yield±SD
A3	50	25	25	20	20	5,815±212	0.906±0.048	21.78±1.75
A4	50	15	35	20	20	7,989±115	0.989±0.032	17.34±2.35
A5	50	35	15	20	20	3,127±106	0.856±0.028	23.73±1021
B3	70	20	10	20	20	915±06	0.325±0.045	27.34±2.45
B4	70	10	20	20	20	1,119±13	0.336±0.033	350.54±1.76
B5	70	25	05	20	20	1,011±11	0.346±0.029	38.46±2.12
C3	80	10	10	20	20	468.3±7.7	0.291±0.022	42.56±2.33
C4	80	05	15	20	20	517.9±6.6	0.286±0.018	41.61±3.46
C5	80	15	05	20	20	318.6±2.3	0.281±0.015	48.63±5.16
D3	85	10	05	20	20	82.46±2.38	0.272±0.028	82.90±3.78
D4	85	05	10	20	20	118.3±2.8	0.289±0.029	80.24±1.17
D5	90	05	05	20	20	615±45	0.346±0.039	72.24±2.13

Values were expressed as mean±standard deviation

PDI polydispersity index, *NIPAM N*-isopropyl acryl amide, *VP* vinyl pyrrolidone, *MBA*, *N*,*N*′-methylene-bis-acrylamide

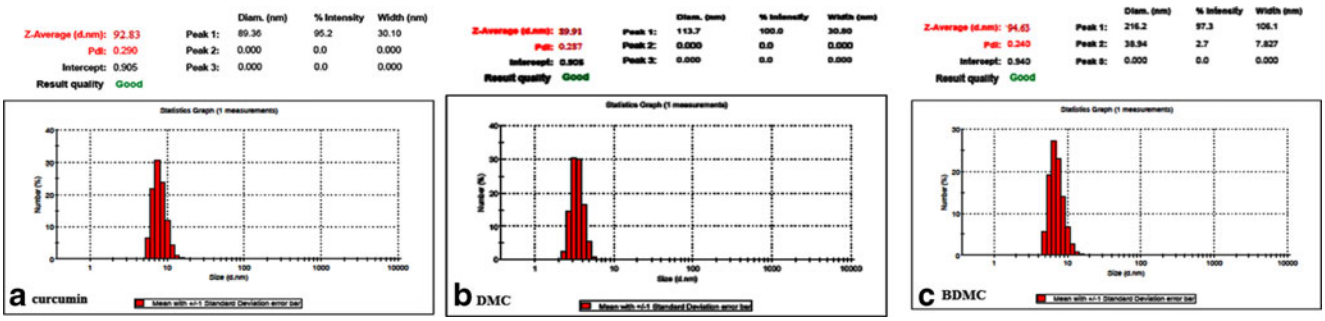

Fig. 1 Dynamic light scattering techniques for determining the particle size of Cur, DMC, and BDMC of particle size

The size of the NPs depends upon the optimum concentration of NIPAM, VP, AA, and MBA and ratio of PNIPAM/MBA. On the basis of particle size (<100 nm) and process yield (<80 %), the formulation code D3 for the placebo PNIPAM NPs having the ratio of PNIPAM/MBA (99.4/0.6) in which the monomers molar ratio is NIPAM/VP/AA (85/10/05) had optimum particle size of 82.46±2.38 nm, PDI of 0.272±0.028, and process yield of 82.90±3.78 in Table 1. Therefore, the nanoformulations containing PNIPAM/MBA ratio of 99.4/0.6 were selected for the preparation of Cur-, DMC-, and BDMC-loaded PNIPAM NPs separately. Cur, DMC, and BDMC dissolved in ethanol (1 mg/mL), gradually added to the co-polymeric solution, and stirred vigorously at room temperature with mild sonication and vortexing up to 1 % *w/w* curcumin w.r.t (i.e., the amount of co-polymeric micelles to give a clear aqueous solution). Cur-, DMC-, and BDMC-loaded PNIPAM NPs were also observed for mean particles size, PDI, zeta potential, and process yield. The mean particle size of Cur-, DMC-, and BDMC-loaded PNIPAM NPs was bigger (92.46±2.8 nm, 91.23±4.2, and 94.28±1.91, respectively) as compared to placebo PNIPAM NPs separately as shown in Fig. 1. So, we observed that the curcuminoids-loaded nanoparticles have less than 100 nm particle size because the drug is entrapped inside the core of placebo nanoparticles, while the placebo nanoparticles have less than 100 nm size; thus, only slight increase in particle size was observed.

The particle size of optimized PNIPAM NPs was also characterized with TEM and the result was found to be less than 100 nm as shown in Fig. 2. Hence, the optimized PNIPAM NPs (D3) was selected for further optimization studies after incorporating the drug. The PNIPAM-Cur, PNIPAM-DMC, and PNIPAM-BDMC NPs separately were prepared and evaluated for process yield, mean particle size, PDI, LC, and EE. The results are shown in Table 2. The process yield, mean particle size, and PDI with different drug polymer ratio were ranged between 81.83±4.69 and 87.23±4.78 %, 92.46±2.8 and 328.24±8.9 nm, and 0.291±0.052 and 0.462±0.064 for the PNIPAM-Cur NPs, 82.06±4.29 and 86.73±4.62 %, 91.23±4.2 and 337.63±7.2 nm, and 0.283±0.063 and 0.469±0.061 for PNIPAM-DMC NPs, and

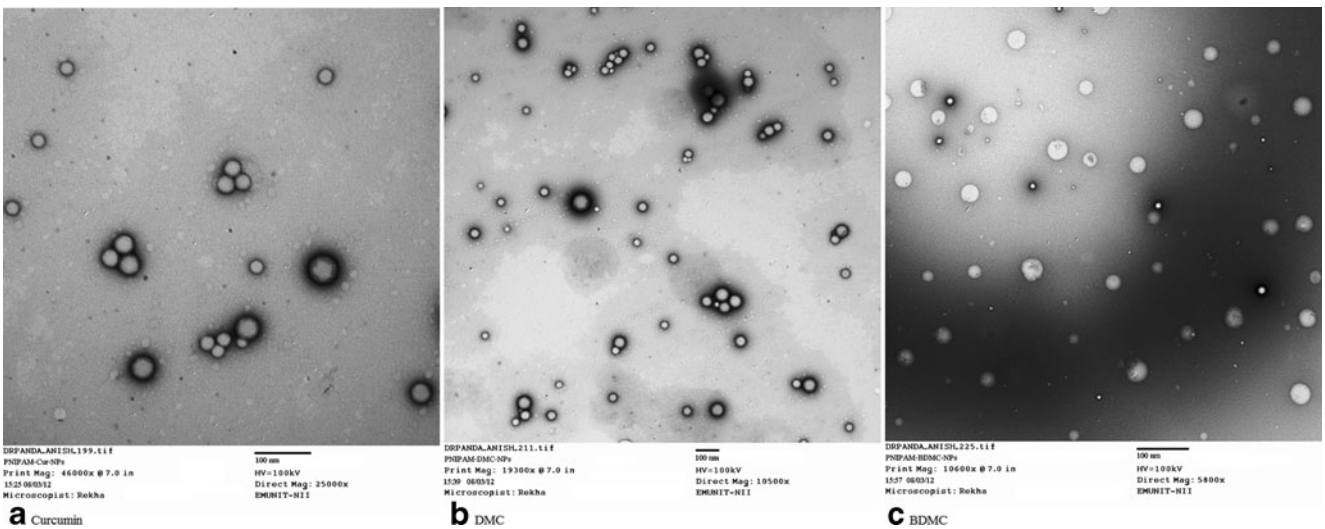

Fig. 2 Transmission electron microscopy (TEM) images of PNIPAM encapsulated with **a** curcumin; **b** demethoxycurcumin; **c** bisdemethoxycurcumin of optimized NPs

Table 2 Optimization of drug polymer ratio of PNIPAM-Cur NPs, PNIPAM-DMC NPs, and PNIPAM-BDMC NPs on the basis of particle size, PDI, zeta potential, process yield, LC, and EE%

Formulation code	Drug/polymer ratio	Mean particle size (nm)±SD	Mean PDI±SD	Process yield±SD	Mean zeta potential (mV)±SD	LC (%)	EE (%)
Cur-PNIPAM-1	1:10	92.46±2.8	0.291±0.052	81.83±4.69	−16.2±1.42	39.31±3.7	84.63±4.2
Cur-PNIPAM-2	2:10	198.74±6.6	0.423±0.042	83.29±5.24	−15.02±2.90.	51.73±2.4	81.24±4.9
Cur-PNIPAM-3	3:10	328.24±8.9	0.462±0.064	87.23±4.78	−12.1±3.16	59.29±2.8	74.13±3.9
DMC-PNIPAM-1	1:10	91.23±4.2	0.283±0.063	82.06±4.29	−15.6±1.33	38.91±3.6	84.71±3.99
DMC-PNIPAM-2	2:10	196.78±6.2	0.429±0.049	84.91±6.11	−14.9±2.78	52.16±2.9	80.33±4.2
DMC-PNIPAM-3	3:10	337.63±7.2	0.469±0.061	86.73±4.62	−13.6±3.76	62.39±3.4	71.23±2.6
BDMC-PNIPAM-1	1:10	94.28±1.91	0.242±0.046	82.29±4.71	−16.6±1.21	40.61±3.6	85.73±4.31
BDMC-PNIPAM-2	2:10	205.53±3.16	0.424±0.046	86.74±2.12	−14.3±2.69	53.23±2.9	82.16±4.62
BDMC-PNIPAM-3	3:10	346.23±6.9	0.472±0.068	88.24±4.18	−12.8±3.27	65.26±4.2	72.93±3.9

All the above nine formulation PNIPAM NPs, PNIPAM/MBA ratio fixed at 99.4/0.6 in which NIPAM/VP/AA::85/10/05

PDI polydispersity index, *SD* standard deviation, *EE* entrapment efficiency, *LC* loading capacity, *PNIPAM* polymeric *N*-isopropyl acryl amide, *Cur* curcumin, *DMC* demethoxycurcumin, *BDMC* bisdemethoxycurcumin, *NPs* nanoparticles

82.29±4.71 and 88.24±4.18 %, 94.28±1.91 and 346.23 ±6.9 nm, and 0.242±0.046 and 0.472±0.068 for PNIPAM-BDMC NPs, respectively. The LC and EE varied for the PNIPAM-Cur-NPs from 39.31±3.7 to 59.29±2.8 % and 84.63±4.2 to 84.63±4.2 %; for the PNIPAM-DMC-NPs from 38.91±3.6 to 62.39±3.4 % and 84.71±3.99 to 71.23±2.6 %; for the PNIPAM-BDMC NPs from 40.61±3.6 to 65.26±4.2 % and 85.73±4.31 to 72.93±3.9 %, which depend upon the drug polymer. Cur-PNIPAM-1, DMC-PNIPAM-1, and BDMC-PNIPAM-1 were selected best optimized formulations due to its optimum particle size, PDI, and process yield shown in Figs. 1 and 2. The surface morphology of PNIPAM NPs recorded from SEM was either spherical or ellipsoidal (Fig. 3).

Effect on locomotor activity

Spontaneous locomotor activity was observed over a period of 10 min for each rat in each group. In the MCA-occluded rats, significant reduction in locomotor count was observed ($p<$ 0.001) as compared to sham group (Fig. 4a). In all groups, pretreated with Cur, DMC, and BDMC (100 μg/kg) intranasal delivery showed improved spontaneous activity when compared to MCAO group. However, PNIPAM nanoformulation of curcumin at a dose of 100 μg/kg was most active.

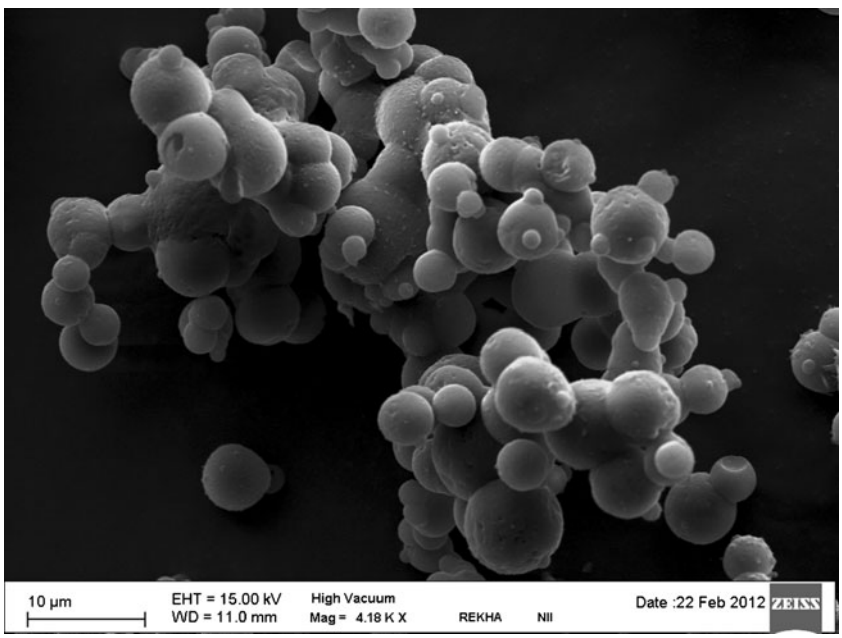

Fig. 3 Scanning electron microscopy images (SEM) of surface morphology of the prepared PNIPAM-NPs

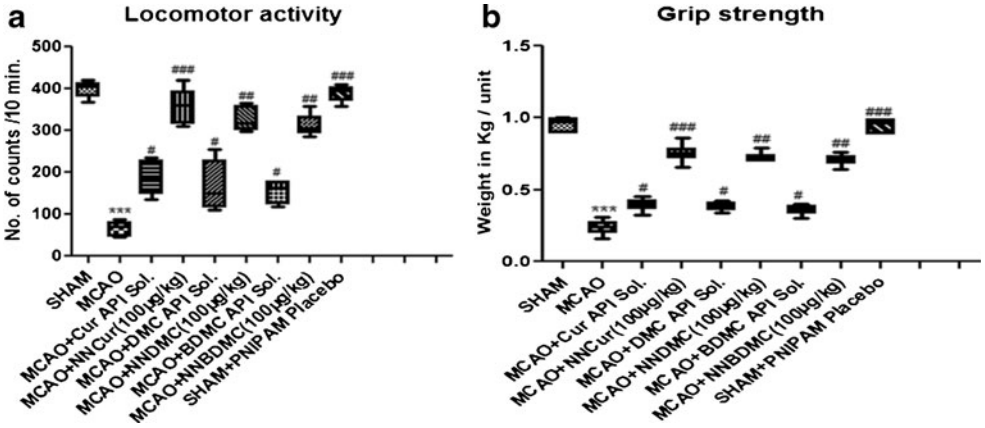

Fig. 4 **a**, **b** Graph showing results of various groups treated with Cur, DMC, and BDMC on locomotor activity, grip strength in middle cerebral artery-occluded (MCAO) rats. Data represented as mean+SEM of six animals. Significance was determined as ***$p<0.001$ when compared with sham group; #$p<0.05$, ##$p<0.01$, ###$p<0.001$ when compared with MCAO group

Effect on grip strength

In the MCAO group, a significant decrease ($p<0.001$) in grip strength was observed as compared to the sham group. Rats pretreated with PNIPAM nanoformulation of Cur, DMC, and BDMC at a dose of 100 μg/kg (Fig. 4b) showed improvement in grip strength when compared with MCAO group significantly.

Pretreatment with Cur, DMC, and BDMC decreased the TBARS level

The effect of Cur, DMC, and BDMC on TBARS level was measured to demonstrate the oxidative damage by lipid peroxidation (LPO) in MCAO group rats. A significant increased ($p<0.001$) level of TBARS was observed in MCAO group animals as compared to sham group. Rats pretreated with Cur, DMC, and BDMC at a dose of 100 μg/kg exhibited significant attenuation in TBARS level as compared to MCAO group rats (Fig. 5). PNIPAM nanoformulation of curcumin at a dose of 100 μg/kg ($p<0.001$) showed the best results when compared among the treated groups.

Effect of Cur, DMC, and BDMC on endogenous antioxidant system

The activities of antioxidant enzymes (GPx, GR, superoxide dismutase (SOD), and catalase) were decreased significantly in MCAO group animals as compared to sham group (Fig. 6) and their activities were protected significantly in groups pretreated with Cur, DMC, and BDMC as compared to MCAO group animals. PNIPAM nanoformulation of curcumin at a dose of 100 μg/kg ($p<0.001$) showed the best results in all the treatment groups.

Morphological changes

Histopathological changes in neuron after ischemia–reperfusion injury were investigated by hematoxylin–eosin staining. The sections of the sham group showed normal cell with no pathologic change, whereas the sections of the MCAO group showed a focus of brain damage with neuronal loss and presence of numerous vacuolated spaces. Intact neurons were absent in that area. The corresponding area in the sections from the PNIPAM nanoformulation of curcumin + MCAO group showed partial neuronal loss with presence of intact neurons in between the vacuolated spaces. PNIPAM nanoformulation of curcumin treatment ameliorated neuronal abnormalities in the PNIPAM nanoformulation of curcumin + MCAO group as compared with the MCAO group animals (Fig. 7).

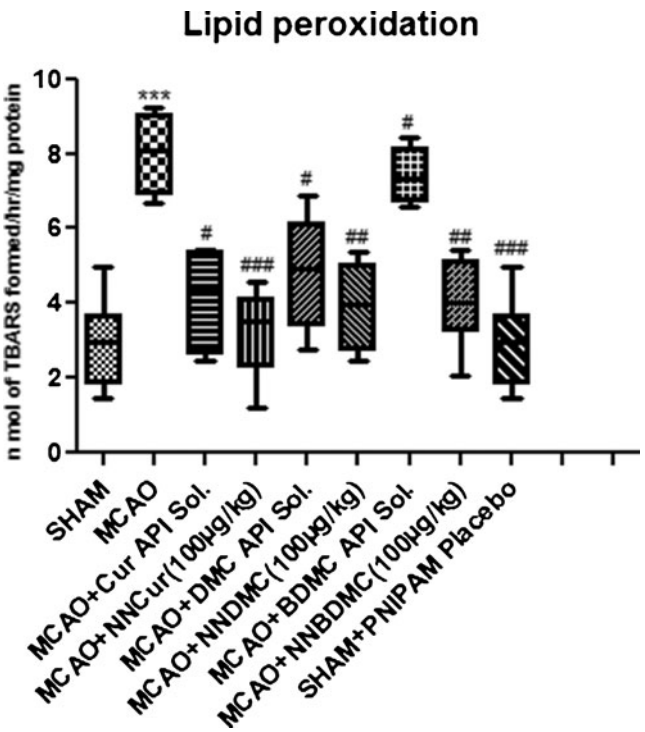

Fig. 5 Effect of PNIPAM nanoformulation of Cur, DMC, and BDMC pretreatment on TBARS content. TBARS content was significantly increased in MCAO group as compared to sham group. Significance was determined as ***$p<0.001$ when compared with sham group; #$p<0.05$, ##$p<0.01$, ###$p<0.001$ when compared with MCAO group

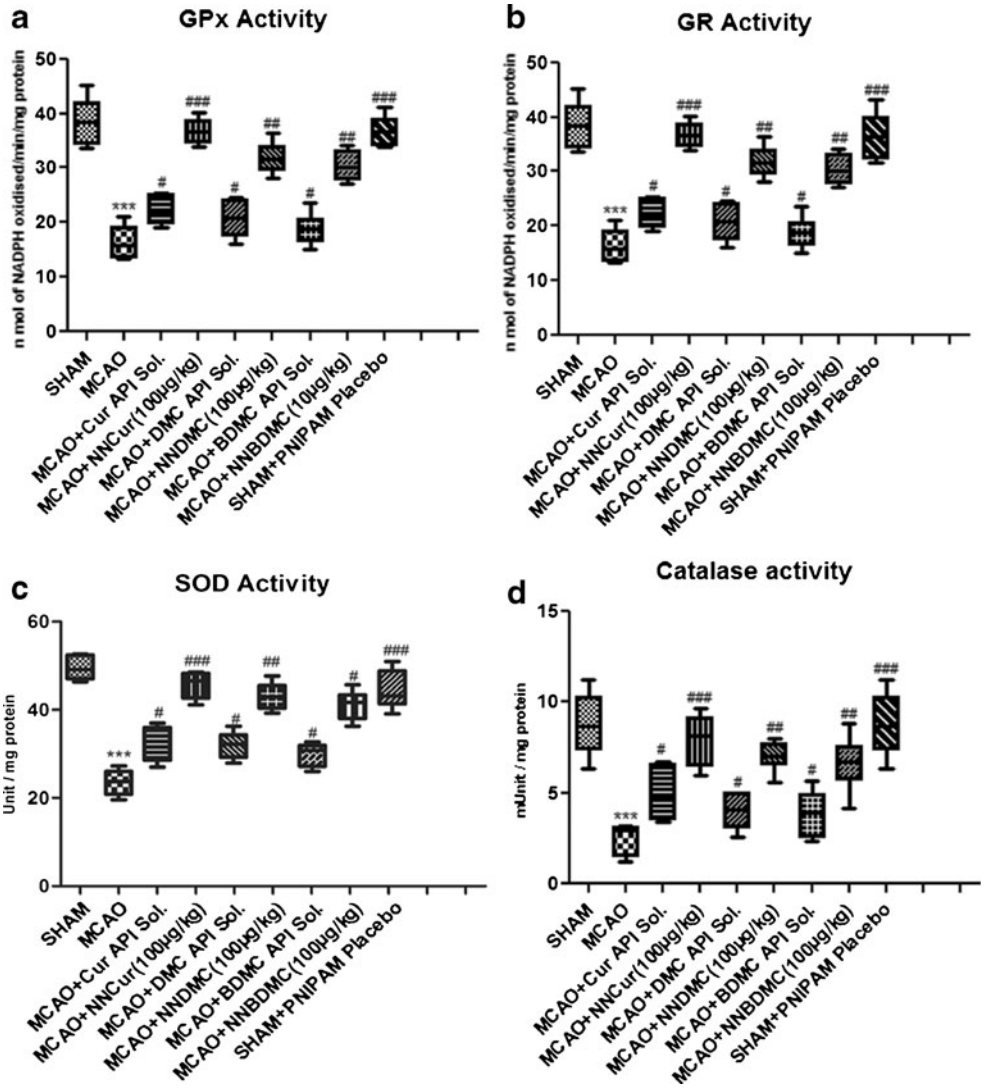

Fig. 6 Effect of PNIPAM nanoformulation of Cur, DMC, and BDMC on the activity of various enzymes in different treated groups. Results were expressed as mean±SEM of six animals. Significance was determined as ***$p<0.001$ when compared with sham group; #$p<0.05$, ##$p<0.01$, ###$p<0.001$ when compared with MCAO group

Discussion

To increase their bioavailability, we incorporate curcuminoids inside the core of PNIPAM polymer. Curcuminoids are encapsulated inside the hydrophobic core to make it safe from degradation from the matrix environment which leads to enhance uptake of curcumin by targeting to the brain. PNIPAM polymeric micelles show high of drug loading with gradient release of curcumin with time. Polymer formed from the vinyl group-containing monomers (e.g., NIPAM, VP, and AA) has amphiphilic character. Isopropyl groups of NIPAM and –CH2–CH2– backbone of the polymer make the hydrophobic segments in the polymer whereas the amide bond of NIPAM, pyrolidone groups of VP, and carboxylic group of AA makes the hydrophilic part within the polymer. So when such a copolymer is dissolved in water, the water-soluble segments get dissolved in water, whereas water-insoluble isopropyl comes together by hydrophobic interactions resulting in the micelles-like structure. In an aqueous environment, the core of the micelles consists of hydrophobic blocks and the shell region consists of hydrophilic blocks. The core of co-poly-(NIPAM–VP–AA) micelles serves as a nonaqueous reservoir for drugs where the drugs are stabilized against chemical modifications.

NIPAM and AA come under the definition of stimuli-responsive polymers and, hence, are termed as intelligent materials. NIPAM exhibits a very sensitive phase transition at approximately 31–38 °C, that is, at their LCST. Below LCST, the polymer is soluble in aqueous media, while it becomes opaque and forms precipitate above LCST (Gang et al. 2009; Ramírez-Fuentes et al. 2008). However, the addition of AA also results in an increase in LCST (Loo-Teck et al. 2005) and the VP rendered a hydrogel and mucoadhesive properties of the polymer (Gang et al. 2009; Robinson et al. 1990; Alsarra et al. 2011).

In the present study, we have critically compared the efficacy of PNIPAM-loaded nanoparticles formulation of Cur, DMC, and BDMC. The most abundant naturally

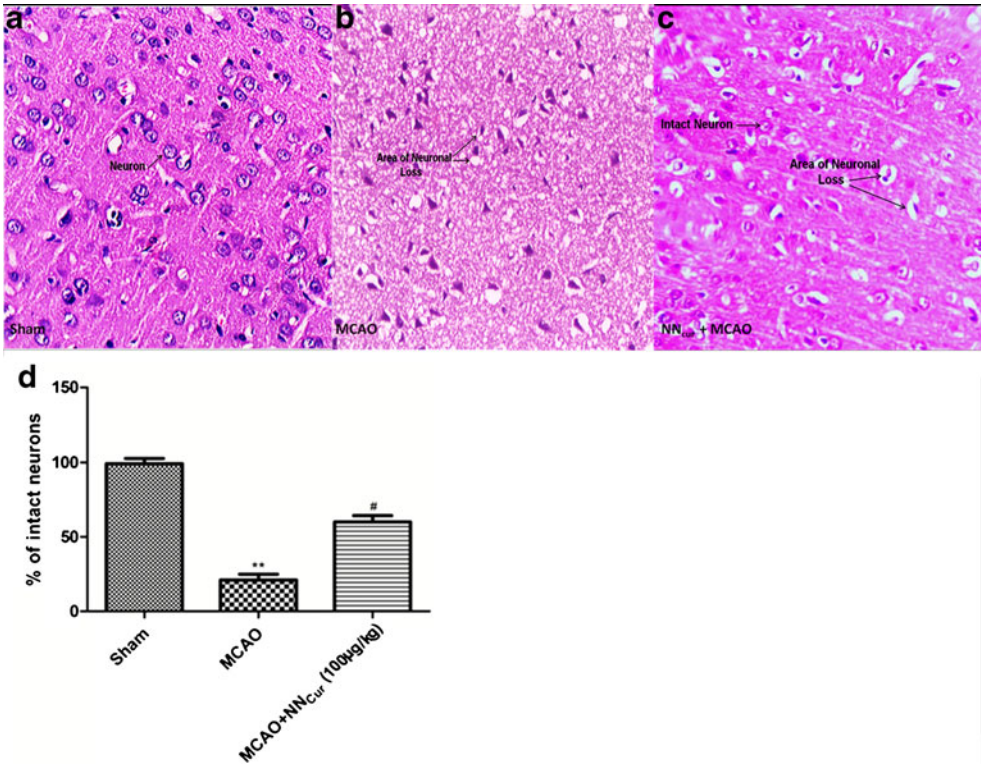

Fig. 7 Effect of PNIPAM nanoformulation of curcumin (NNcur at 100 μg/kg) administration on hematoxylin and eosin staining in the brain sections of the sham, MCAO, and NNcur + MCAO groups. **a** Cortical area of sham group animal showed uniform distribution of neurons. Normal neurons with the characteristic conical outlines with no abnormal features are seen. **b** Tissues around infarcted area in the MCAO group show a focal area of vacuolation and neuronal loss. **c** The NNcur + MCAO group rats show partial neuronal loss. **d** Quantification of neuronal damage of sham, MCAO, and NNcur + MCAO groups. Original magnification ×20 and *scale bar* = 20 μm

occurring phenolic compound isolated from *C. longa* as a potential of a new prophylactic anti-oxidative and anti-apoptotic target in cerebral stroke. Characteristically, ischemic–reperfusion-induced brain injury is associated with oxidative stress and behavioral alterations which is seen to be well ameliorated with the pretreatment of PNIPAM nanoparticles formulation of curcuminoids (Cur, DMC, and BDMC). Herein, we observed that curcumin (at a dose of 100 μg/kg)-loaded PNIPAM nanoparticles prevents cerebral ischemia–reperfusion injury by ameliorating oxidative damage significantly as compared to other curcuminoids (DMC and BDMC)-loaded PNIPAM nanoparticles. This may be due to presence of phenolic group, as curcumin contains two phenyl methoxy groups; DMC contains one and no phenolic group in BDMC (Sandur et al. 2007). The better antioxidant activity of PNIPAM nanoformulation of curcuminoids may also depend on *ortho*- and *meta*-position of functional group.

Experimental models of stroke have been developed in animals in an attempt to mimic the events of human cerebral ischemia and to investigate the pathology of cerebral ischemia. Free radicals are known to play key role in neurobehavioral deficit in experimental models through oxidative stress (Fukui et al. 2002). The poor neurobehavioral outcome in ischemic group may be due to free radical generation, which alters locomotion and motor coordination due to the necrosis induced in sensorimotor cortices and caudate-putamen (Hunter et al. 1998) which has a command on motor and sensorimotor activities. The locomotor and grip strength have indicated that vehicle injection did not cause deterioration of

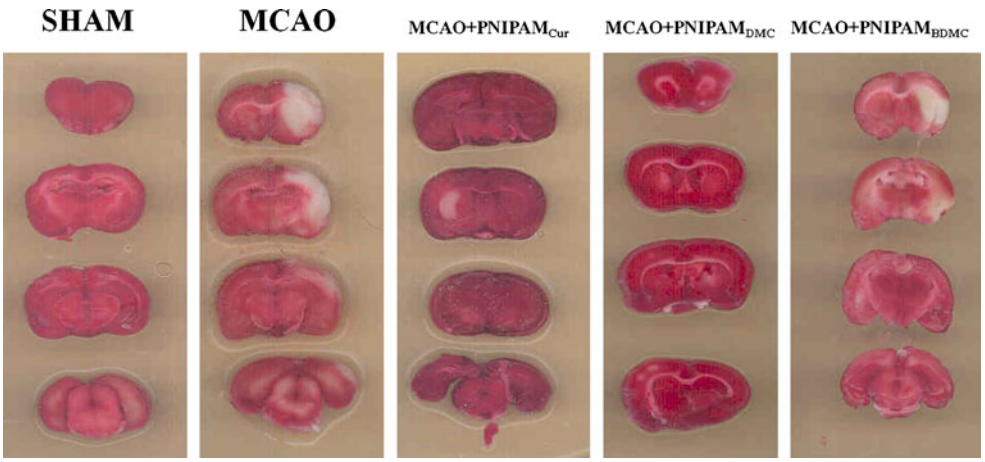

Fig. 8 PNIPAM-Cur, DMC, and BDMC NPs pretreatment for 21 days improves performances in the neurological deficits after stroke: Representative photographs of brain sections stained with 0.1 % TTC stain of Sham, MCAO, $PNIPAM_{Cur}$, $PNIPAM_{DMC}$, and $PNIPAM_{BDMC}$ brain sections

motor performance in the rats, while the MCAO group showed depletion in locomotion and poor coordination.

Functional deficits are common neurologic sequel in patients with brain injuries and animal models of cerebral ischemia. Earlier studies have shown an improvement in various behavioral outputs as a result of antioxidant treatment. Neuroprotective effects of curcumin suggest that it is a powerful antioxidant, corroborating previous studies (Sandur et al. 2007). PNIPAM nanoparticles formulation of curcumin seems to protect against oxidative stress by decreasing lipid peroxidation, a sensitive marker of oxidative damage. The mechanisms manifested to overcome the stress induced by prooxidants includes the following: enhanced protein synthesis, scavenging free radicals (Locher et al. 1998), increase in glutathione (GSH) content (Avci et al. 2012), and preservation of cell membrane integrity (Dehmlow et al. 1996). Oxidative stress-induced biochemical alterations are well known in ischemia–reperfusion brain injury. Cells have evolved elaborated systems, including enzymatic and non-enzymatic systems to cope with various forms of oxidative stress. ROS are threatened to neuronal survival by their ability to propagate the initial attack on lipid-rich membranes of the brain to cause LPO (Kale et al. 1999). However, the cell damage can be prevented by detoxification of free radicals, which eventually prevent the progress of LPO. We have observed an elevated level of LPO in the form of TBARS accompanied by depleted content of GSH which are in agreement with the previous study (Zafar et al. 2003). As all antioxidant defenses are interconnected (Sun et al. 2009); hence, disruption of one would disrupt the whole microenvironment. The ischemia–reperfusion causes an overproduction of free radicals which, in turn, causes oxidative damages to membrane's lipid and protein levels and ultimately leads to a decrease in the content of GSH and activity of its dependent enzyme (GPx and GR) activity along with SOD. This oxidative neuronal damage in ischemic brain insult is consistent with previous reports (Khuwaja et al. 2011). Superoxide or its derivatives have been shown to damage or destroy cells in a variety of ways in ischemic–reperfusion insult. It is well appreciated that, under ischemia, free radical burden is primarily contained by SOD. Prophylactic administration of PNIPAM nanoparticles formulation of curcumin prior to ischemia–reperfusion injury significantly increased SOD activity, probably by utilizing the production of superoxide radicals ($O^{\cdot 2-}$) which was produced during ischemia–reperfusion. This decrement and the other biochemical parameters were reflected in histological analysis, confirming the protective effects of the nanoformulation of curcumin. However, no significant alteration was observed in the curcuminoids API solution group as compared with the MCAO group. No significant change was observed between the PNIPAM placebo nanoparticles + pretreated sham group and the sham group. TTC stain of sham, MCAO, PNIPAM-Cur, PNIPAM-DMC, and PNIPAM-BDMC brain sections showed reproducible and readily detectable lesions in the areas that are supplied by the MCA after 22 h of reperfusion (Fig. 8).

Conclusion

Our result showed that curcumin (100 μg/kg body weight)-loaded PNIPAM nanoparticles are more potent as compared to other curcuminoids (DMC and BDMC) in the treatment of MCAO-induced focal cerebral ischemia in rats. We also concluded that intranasal administration of curcumin-loaded PNIPAM nanoparticles, which could bypass the BBB and enter the brain preferentially, reducing unwanted systemic effects, appears to be a promising strategy for treating cerebral ischemia. Intranasal drug delivery system offered an improvement in nose-to-brain drug delivery since they are able to protect the encapsulated drug from biological and/or chemical degradation, and extracellular transport by P-glycoprotein efflux proteins. This would increase CNS availability of the drug. These observations suggest that PNIPAM-loaded curcumin nanoparticles may also be a potential neuroprotective agent against a variety of conditions where cellular damage is a consequence of oxidative stress.

Acknowledgments The authors are thankful to the Council for Scientific and Industrial Research, Pusa Road, New Delhi, for the granting CSIR-SRF which supported this study.

Conflict of interest Authors have no conflict of interest in this paper. The author (Niyaz Ahmad) is grateful to the Council for Scientific and Industrial Research, Pusa Road, New Delhi, for financial grant of this research.

Animal study Experiments were conducted in accordance with Hamdard Institutional Ethics Committee (JH/FP/0847/2012). Approval for the animal study was given by Institutional Animal Ethical Committee.

References

Akhtar M, Pillai K, Vohora D (2008) Effect of thioperamide on oxidative stress markers in middle cerebral artery occlusion model of focal cerebral ischemia in rats. Hum Exp Toxicol 27:761–767

Ali A, Ahmad FJ, Pillai KK, Vohora D (2004) Evidence of the antiepileptic potential of amiloride with neuropharmacological benefits in rodent models of epilepsy and behavior. Epilepsy Behav 5:322–328

Allen CL, Bayraktutan U (2009) Oxidative stress and its role in the pathogenesis of ischaemic stroke. Int J Stroke 4:461–470

Alsarra IA, Hamed AY, Alanazi FK, Neau SH (2011) Rheological and mucoadhesive characterization of poly(vinylpyrrolidone) hydrogels designed for nasal mucosal drug delivery. Arch Pharm Res 34(4):573–582. doi:10.1007/s12272-011-0407-6

Anand P, Nair HB, Sung B, Kunnumakkara AB, Yadav VR, Tekmal RR, Aggarwal BB (2010) Design of curcumin-loaded PLGA

nanoparticles formulation with enhanced cellular uptake, and increased bioactivity in vitro and superior bioavailability in vivo. Biochem Pharmacol 79:330–338

Ashafaq M, Khan MM, Raza SS, Ahmad A, Khuwaja G, Javed H, Khan A, Islam F, Siddiqui MS, Safhi MM (2012) S-allyl cysteine mitigates oxidative damage and improves neurologic deficit in a rat model of focal cerebral ischemia. Nutr Res 32:133–143

Avci G, Kadioglu H, Sehirli AO, Bozkurt S, Guclu O, Arslan E, Muratli SK (2012) Curcumin protects against ischemia/reperfusion injury in rat skeletal muscle. J Surg Res 172:39–46

Badary OA, Taha RA, Gamal el-Din AM, Abdel-Wahab MH (2003) Thymoquinone is a potent superoxide anion scavenger. Drug Chem Toxicol 26:87–98

Berner MD, Sura ME, Alves BN Jr, Hunter KW (2005) IFN-gamma primes macrophages for enhanced TNF-alpha expression in response to stimulatory and non-stimulatory amounts of microparticulate beta-glucan. Immunol Lett 98:115–122

Bradford MM (1976) A rapid and sensitive method for the quantitation of microgram quantities of protein utilizing the principle of protein-dye binding. Anal Biochem 72:248–254

Dehmlow C, Erhard J, de Groot H (1996) Inhibition of Kupffer cell functions as an explanation for the hepatoprotective properties of silibinin. Hepatology 23:749–754

Fukui K, Omoi NO, Hayasaka T, Shinnkai T, Suzuki S, Abe K, Urano S (2002) Cognitive impairment of rats caused by oxidative stress and aging, and its prevention by vitamin E. Ann N Y Acad Sci 959:275–284

Gang L, Pandya DP, Seong SS (2009) Thermoresponsive core polystyrene–shell NIPAm microgels. Int J Polymer Anal Charact 14:351–363. doi:10.1080/10236660902875208

Hanson LR, Frey WH (2008) Intranasal delivery bypasses the blood–brain barrier to target therapeutic agents to the central nervous system and treat neurodegenerative disease. BMC Neurosci 9:S5

Hunter AJ, Mackay KB, Rogers DC (1998) To what extent have functional studies of ischaemia in animals been useful in the assessment of potential neuroprotective agents? Trends Pharmacol Sci 19:59–66

Iida M, Miyazaki I, Tanaka K, Kabuto H, Iwata-Ichikawa E, Ogawa N (1999) Dopamine D2 receptor-mediated antioxidant and neuroprotective effects of ropinirole, a dopamine agonist. Brain Res 838:51–59

Jayaprakasha GK, Jaganmohan Rao L, Sakariah KK (2006) Antioxidant activities of curcumin, demethoxycurcumin and bisdemethoxycurcumin. Food Chem 98:720–724

Kale M, Rathore N, John S, Bhatnagar D (1999) Lipid peroxidative damage on pyrethroid exposure and alterations in antioxidant status in rat erythrocytes: a possible involvement of reactive oxygen species. Toxicol Lett 105:197–205

Khan MM, Ahmad A, Ishrat T, Khuwaja G, Srivastawa P, Khan MB, Raza SS, Javed H, Vaibhav K, Khan A, Islam F (2009) Rutin protects the neural damage induced by transient focal ischemia in rats. Brain Res 1292:123–135

Khuwaja G, Khan MM, Ishrat T, Ahmad A, Raza SS, Ashafaq M, Javed H, Khan MB, Khan A, Vaibhav K, Safhi MM, Islam F (2011) Neuroprotective effects of curcumin on 6-hydroxydopamine-induced Parkinsonism in rats: behavioral, neurochemical and immunohistochemical studies. Brain Res 1368:254–263

Kim Y, So HS, Kim JK, Park C, Lee JH, Woo WH, Cho KH, Moon BS, Park R (2007) Anti-inflammatory effect of oyaksungisan in peripheral blood mononuclear cells from cerebral infarction patients. Biol Pharm Bull 30:1037–1041

Lannert H, Hoyer S (1998) Intracerebroventricular administration of streptozotocin causes long-term diminutions in learning and memory abilities and in cerebral energy metabolism in adult rats. Behav Neurosci 112:1199–1208

Locher R, Suter PM, Weyhenmeyer R, Vetter W (1998) Inhibitory action of silibinin on low density lipoprotein oxidation. Arzneimittelforschung 48:236–239

Longa EZ, Weinstein PR, Carlson S, Cummins R (1989) Reversible middle cerebral artery occlusion without craniectomy in rats. Stroke 20:84–91

Loo-Teck N, Hiroshi N, Isao K, Kumao U (2005) Photocuring of stimulus responsive membranes for controlled-release of drugs having different molecular weights Radiat. Phys Chem 73–117

Mistry A, Stolnik S, Illum L (2009) Nanoparticles for direct nose-to-brain delivery of drugs. Int J Pharm 379:146–157

Mohandas J, Marshall JJ, Duggin GG, Horvath JS, Tille DJ (1984) Differential distribution of glutathione and glutathione-related enzymes in rabbit kidney. Possible implications in analgesic nephropathy. Biochem Pharmacol 33:1801–1807

Naha PC, Casey A, Tenuta T, Lynch I, Dawson KA, Byrne HJ, Davoren M (2009) Preparation, characterization of NIPAM and NIPAM/BAM copolymer nanoparticles and their acute toxicity testing using an aquatic test battery. Aquat Toxicol 92:146–154

Ohkawa H, Ohishi N, Yagi K (1979) Assay for lipid peroxides in animal tissues by thiobarbituric acid reaction. Anal Biochem 95:351–358

Ramírez-Fuentes YS, Bucio E, Burillo G (2008) Thermo and pH sensitive copolymer based on acrylic acid and *N*-isopropylacrylamide grafted onto polypropylene. Polym Bull 60:79–87. doi:10.1007/s00289-007-0827-0

Raza SS, Khan MM, Ahmad A, Ashafaq M, Khuwaja G, Tabassum R, Javed H, Siddiqui MS, Safhi MM, Islam F (2011) Hesperidin ameliorates functional and histological outcome and reduces neuroinflammation in experimental stroke. Brain Res 1420:93–105

Robinson BR, Sullivan FM, Borzelleca JF (1990) In: Schwartz SL (ed) A critical review of kinetics and toxicology of PVP (povidone). Lewis, Chelsea

Sandur SK, Pandey MK, Sung B, Ahn KS, Murakami A, Sethi G, Limtrakul P, Badmaev V, Aggarwal BB (2007) Curcumin, demethoxycurcumin, bisdemethoxycurcumin, tetrahydrocurcumin and turmerones differentially regulate anti-inflammatory and anti-proliferative responses through a ROS-independent mechanism. Carcinogenesis 28:1765–1773

Somparn P, Phisalaphong C, Nakornchai S, Unchern S, Morales NP (2007) Comparative antioxidant activities of curcumin and its demethoxy and hydrogenated derivatives. Biol Pharm Bull 30:74–78

Sun M, Zhao Y, Gu Y, Xu C (2009) Inhibition of nNOS reduces ischemic cell death through down-regulating calpain and caspase-3 after experimental stroke. Neurochem Int 54:339–346

Thiyagarajan M, Sharma SS (2004) Neuroprotective effect of curcumin in middle cerebral artery occlusion induced focal cerebral ischemia in rats. Life Sci 74:969–985

Thiyagarajan M, Kaul CL, Sharma SS (2004) Neuroprotective efficacy and therapeutic time window of peroxynitrite decomposition catalysts in focal cerebral ischemia in rats. Br J Pharmacol 142:899–911

Umar S, Zargan J, Umar K, Ahmad S, Katiyar CK, Khan HA (2012) Modulation of the oxidative stress and inflammatory cytokine response by thymoquinone in the collagen induced arthritis in Wistar rats. Chem Biol Interact 197:40–46

Xu FJ, Kang ET, Neoh KG (2006) pH- and temperature-responsive hydrogels from crosslinked triblock copolymers prepared via consecutive atom transfer radical polymerizations. Biomaterials 27:2787–2797

Yang KY, Lin LC, Tseng TY, Wang SC, Tsai TH (2007) Oral bioavailability of curcumin in rat and the herbal analysis from *Curcuma longa* by LC-MS/MS. J Chromatogr B Analyt Technol Biomed Life Sci 853:183–189

Zafar KS, Siddiqui A, Sayeed I, Ahmad M, Salim S, Islam F (2003) Dose-dependent protective effect of selenium in rat model of Parkinson's disease: neurobehavioral and neurochemical evidences. J Neurochem 84:438–446